

GIANT MAGNETORESISTANCE IN MAGNETIC NANOSTRUCTURES

S. S. P. Parkin

IBM Research Division, Almaden Research Center, 650 Harry Road,
San Jose, California 95120

KEY WORDS: multilayers, granular metals, interlayer exchange coupling,
magnetic recording, sputtered films

ABSTRACT

This chapter contains a brief review of the giant magnetoresistance (GMR) effect exhibited by magnetic multilayers, granular alloys, and related materials. Subjects covered include a description of the phenomenon, and the related oscillatory interlayer exchange coupling in magnetic multilayers; a simple model of giant magnetoresistance; the inverse GMR effect in spin-engineered magnetic multilayers; structures that display large changes in resistance in small magnetic fields, possibly for use in magnetic field sensors; and the dependence of GMR on various aspects of the magnetic structures.

INTRODUCTION

There has been much interest in recent years in artificially engineered nano-structured materials with novel physical properties. One area of particular interest is that of metal multilayers. These materials have been studied for the past 30 years or more, but it is only relatively recently that detailed expertise has been developed to prepare and sufficiently characterize the structure of such materials (1-3). Metal multilayers have been studied for their novel superconducting properties, for the possibility of creating metals much stronger and tougher than the individual components of the multilayer, for creating super-mirrors for X-ray or neutron scattering monochromators, and for a host of other reasons. Most recently, interest in metal multilayers has centered on multilayers comprised of

thin magnetic layers separated by thin nonferromagnetic layers. These multilayers display unusual magnetic and transport properties that are the subject of this brief review. Note that several excellent comprehensive reviews of the transport and magnetic properties of magnetic multilayers and related materials are available (4–10).

Usually the change in resistance of thin metal films with application of a magnetic field is small (11). However, in 1988 it was found that single crystalline (100)-oriented Fe/Cr/Fe sandwiches (12) and (100)-oriented Fe/Cr multilayers (13) displayed much larger magnetoresistance values than could be accounted for by the magnetoresistance of the individual Fe layers themselves. The resistance of the multilayers was found to decrease by almost a factor of two when a field of ≈ 20 kOe was applied at low temperatures (4.2 K) (13). The term giant magnetoresistance (GMR) was coined to describe this effect. The thickness of the Cr layers in these structures was chosen to correspond to the thickness that was previously found to give rise to an unusual antiferromagnetic interlayer exchange coupling of neighboring Fe layers (14, 15). These films were prepared by molecular beam epitaxy (MBE) (see, for example, 16–18), which is a sophisticated and expensive ultra-high vacuum deposition technique. Soon it was shown that similar GMR results could be obtained in polycrystalline Fe/Cr sandwiches and multilayers prepared using inexpensive and simpler sputter-deposition methods (19, 20). Sputter-deposition allowed for the study of a wide variety of metal multilayers, and this led to the surprising discovery that GMR was common to many metal multilayers (19, 21). To date, the largest GMR effects at room temperature are found in Co/Cu multilayers comprised of thin Co and Cu layers (21–23).

Interest in transition metal multilayers has also been greatly increased in recent years with the discovery of oscillations in the interlayer magnetic exchange coupling in multilayers comprised of thin ferromagnetic layers of Fe, Co, Ni, and their various alloys separated by thin layers of virtually all the nonferromagnetic transition and noble metals (19, 22, 24, 25). This discovery led to the prospect of artificially engineering multilayered structures with complex magnetic structures, useful both for understanding the physics of these materials as well as for technological applications. Indeed, magnetic thin film structures already have found important applications for storing information in magnetic and magneto-optical disk storage devices (26, 27), for magnetic field sensors in magnetic recording magnetoresistive read heads (28), and for nonvolatile random access memory (29). Applications involving hybrid magnetic/semiconductor structures have been proposed (30), and recently, spin switches, devices based on transport of spin-polarized electrons across magnetic/nonmagnetic interfaces, have been devised and prototypes built (31, 32).

It is likely that devices based on the giant magnetoresistance phenomenon will be used within a few years.

GIANT MAGNETORESISTANCE

Magnetic Multilayers: Polycrystalline Co/Cu and Fe/Cr

Figure 1 shows plots of the change in room temperature resistance ΔR vs in-plane magnetic field for two polycrystalline multilayers of Fe/Cr and

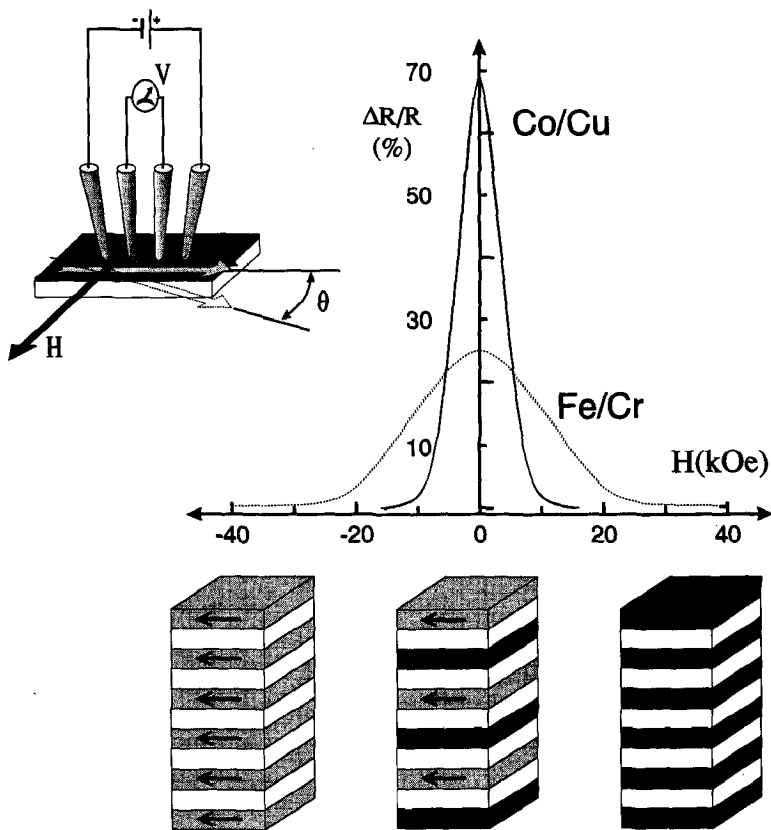


Figure 1 Room temperature resistance vs in-plane magnetic field curves for polycrystalline Fe/Cr and Co/Cu multilayers deposited by magnetron sputtering (for detailed deposition conditions, see 19, 21, but note that the Co/Cu multilayer was deposited at 2.1 mTorr). The measurement geometry is shown schematically in the top left corner. The magnetic state of the antiferromagnetically coupled multilayers is shown schematically in the lower portion of the figure for large negative, zero, and large positive magnetic fields.

Co/Cu, respectively¹. Note that the resistance is measured with the current in the plane of the layers, and the magnetic field is applied orthogonal to the current also in the plane of the layers. At high magnetic fields, the resistance saturates at some value R , and the sample resistance is normalized to this value. The figure shows that the resistance of the multilayers is significantly higher in small fields as compared with high fields. The variation in resistance is related to a change in the relative orientation of neighboring ferromagnetic Fe or Co layers with applied magnetic field. The resistance is higher when adjacent magnetic layers are aligned antiparallel to one another, as compared with parallel alignment, shown schematically in cartoons of the magnetic multilayer included in Figure 1. In the figure, values of room-temperature saturation magnetoresistance $\Delta R/R$ of more than 25 and 70% are observed for Fe/Cr and Co/Cu, respectively, with corresponding saturation fields of ≈ 25 and 10 kOe. The corresponding GMR values at 4.2 K are significantly higher at 110 and 130%, respectively.

The GMR of the samples shown in Figure 1 are some of the highest recorded GMR values in magnetic multilayers. Higher values still have been reported in single crystalline (100) Fe/Cr multilayers. GMR values exceeding 150% at 4.2 K have been found in magnetron-sputtered samples (33), and values of more than 220% at 1.5 K have been reported recently in MBE-deposited multilayers (34).

As shown schematically in Figure 1, the magnetic moments of successive magnetic layers in the Co/Cu and Fe/Cr multilayers are arranged antiparallel to one another in small fields. This is a consequence of an antiferromagnetic interlayer exchange coupling J_{AF} propagated through the intervening Cr or Cu layers. As the Cr or Cu layer thickness is varied, the exchange coupling of the magnetic layers is found to vary in sign, oscillating between antiferromagnetic (AF) and ferromagnetic (F) coupling (19, 22). This is manifested, for example, as an oscillation in the magnitude of the GMR effect with increasing separation of the magnetic layers and

¹ The structures of the Fe/Cr and Co/Cu multilayers shown in Figure 1 are as follows: Si/40ÅCr/[8ÅFe/7.5ÅCr]₃₉/8ÅFe/15ÅCr, and Si/50ÅFe/[8ÅCo/7.5ÅCu]₅₉/8ÅCo/20ÅFe. Both multilayers were deposited on Si(100), which was covered with a thin (≈ 10 – 15 Å thick) native oxide layer. The Fe/Cr multilayer was deposited at 125°C, which was found to give rise to maximal GMR values (20). It was postulated that this was a result of reducing the bulk resistivity of the Fe and Cr layers while limiting intermixing of the Fe and Cr layers. The Co/Cu multilayer was deposited at room temperature because deposition at any higher temperature appears to decrease GMR, presumably because of dissolution or intermixing of the Co and Cu layers (21–23). An Fe buffer layer is used. It was discovered that Fe buffer layers give the largest GMR values in Co/Cu multilayers grown on silicon for thin Cu layers (21, 22).

was first observed in sputtered Fe/Cr multilayers (19). Figure 2 gives results for a series of Co/Cu multilayers in which the magnitude of the saturation magnetoresistance is found to oscillate with increasing Cu spacer layer thickness with an oscillation period of $\approx 9 \text{ \AA}$. Large GMR values are found for Cu layer thicknesses for which the Co layers are coupled antiferromagnetically (see Figure 2). For strong ferromagnetic coupling of the Co layers, the relative magnetic alignment of the Co layers is unaffected by magnetic field, and consequently there is no GMR effect. Note that for polycrystalline multilayers, as shown in Figure 2, a significant background magnetoresistance (MR) effect is superimposed on the GMR oscillations. This effect is most likely a consequence of the crystallographic structure of the multilayer, which is comprised of small crystalline grains, typically 100 to 200 \AA in size (35). Although the grains are preferentially oriented along (111), the texture is poor, and there is a considerable angular dispersion of the $\langle 111 \rangle$ axis from grain to grain. In addition, there may also be (100)-oriented grains (36). Because the period of the oscillatory coupling in Co/Cu depends on crystallographic orientation (37, 38), it is possible that GMR oscillations from differently oriented grains in the polycrystalline Co/Cu structures could be superimposed, perhaps accounting for the GMR background shown in Figure 2. For very thick Cu layers, where the interlayer coupling is very weak, GMR is still observed if the magnetic layers break up into magnetic domains, as shown schematically

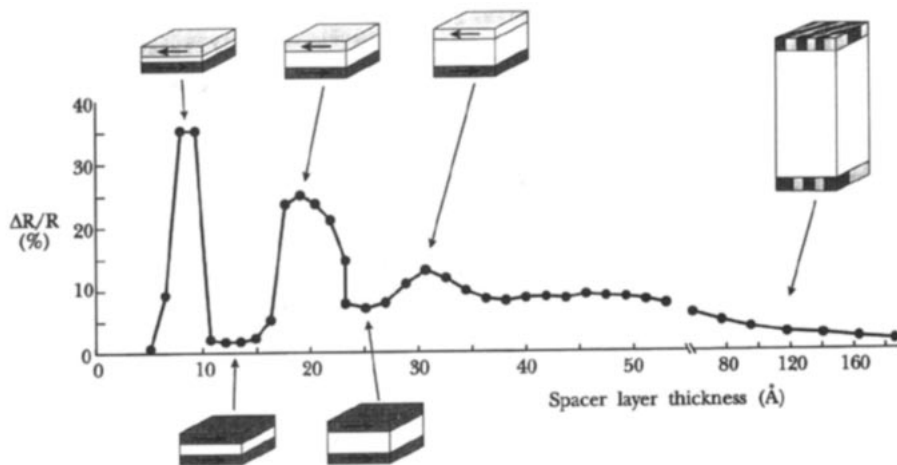


Figure 2 Room temperature saturation magnetoresistance vs Cu spacer layer thickness for a series of polycrystalline sputter-deposited Co/Cu multilayers (from 22). The magnetic state of the multilayer is shown schematically for various Cu layer thicknesses (only two magnetic layers are shown).

in Figure 2. GMR is the result of electrons propagating from one magnetic layer to another magnetic layer for which the magnetic moments are not aligned with one another. Thus there is a certain probability that electrons emanating from a magnetic domain in one magnetic layer will propagate and undergo scattering in a magnetic domain in a neighboring layer (or indeed even in the same layer), which would lead to an increased resistance. The resistance is highest in this case when the net magnetic moment of each layer is close to zero at the coercive field H_c . This leads to twin peaks in resistance at $\pm H_c$.

Granular Alloys—An Example: [111]-Oriented CoCu

The preceding discussion of GMR in uncoupled Co/Cu multilayers indicates that magnetically coupled multilayers are not a prerequisite for the observation of GMR. The layered geometry is also unnecessary, and giant magnetoresistance has been observed in a variety of inhomogeneous magnetic systems. The only requirement is that the system contains a distributed magnetic component in which the relative orientation of the magnetic moments of small magnetic entities will vary with magnetic field or any other variable (such as, for example, temperature or strain). Granular alloys containing magnetic particles in a metallic host bear a strong resemblance to magnetic multilayers, and GMR has been observed in a variety of magnetic granular systems predominantly comprised of Fe, Co, Ni, and their various alloys in Cu, Ag, and Au matrices (39–42) (for a review see C L Chien, this volume). Figure 3 shows typical GMR results for a single crystalline (111)-oriented $\text{Co}_{28}\text{Cu}_{72}$ granular alloy prepared by MBE (41). Resistance vs field curves are shown for the magnetic field applied both in-plane and orthogonal to the sensing current and perpendicular to the plane of the film. There is a significant magnetic anisotropy, perhaps resulting from the shape of the Co particles, or from the intrinsic magnetic anisotropy of the Co itself. Note also that the resistance of the sample is dependent on the magnetic field history. As a result of the considerable magnetic anisotropy, the coercive fields are very different for field applied in the plane of and perpendicular to the plane of the samples. Just as for the uncoupled Co/Cu multilayers described above, the largest resistance in granular alloys is found when the magnetization is close to zero at $\pm H_c$. This corresponds to the state of maximal anti-alignment of the magnetic moments of neighboring magnetic particles. Thus, because the coercive field depends on field orientation, the sample resistance in zero field can be varied by up to a factor of two, as shown in Figure 3. In this case, the sample was first magnetized perpendicular to the film. After reducing the field to zero, the sample was rotated so that the field was aligned in the plane of the sample. Magnetizing the sample

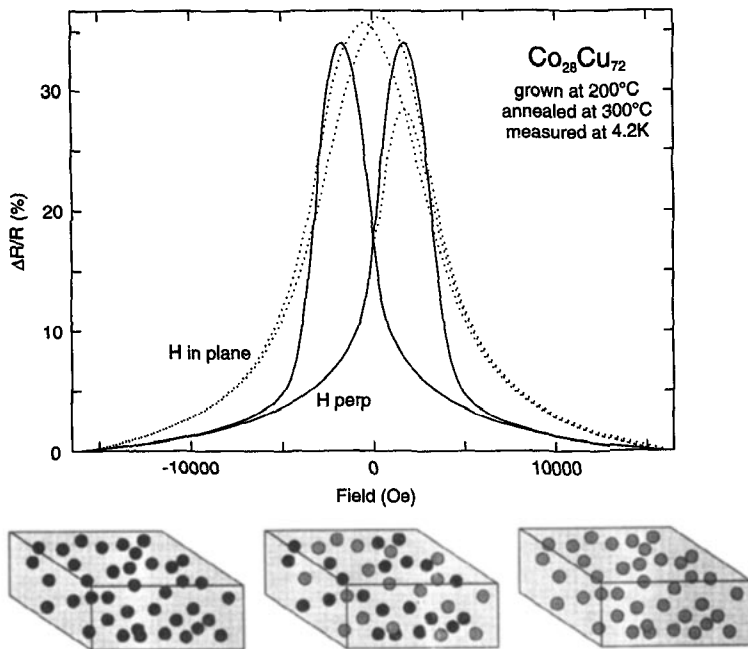


Figure 3 Resistance vs field curves for a MBE-deposited crystalline (111)-oriented $\text{Co}_{28}\text{Cu}_{72}$ alloy. The film was deposited at 200°C and annealed for 1 h at 300°C (for deposition conditions, see 41). Data are shown at 4.2 K for field applied in-plane (and orthogonal to the sense current) and for field applied along the field normal. The arrangement of the magnetic Co particles is shown schematically in the bottom portion of the figure for large negative, zero, and large positive magnetic fields.

and reducing the field to zero results in an increase of the zero field resistance by 51%!

OSCILLATORY INTERLAYER COUPLING

The Cu or Cr in the layers adjacent to the Co or Fe magnetic layers shown in Figure 1 becomes spin-polarized, and these atoms develop magnetic moments. For Cu, the *d*-spin-induced moment, which is parallel to the Co moment, is very small and is about 100 times smaller than the moment on Co itself, as deduced from X-ray magnetic circular dichroism studies (XMCD) (43). For Cr, the induced *d*-moment, which is antiparallel to the Fe moment (44), is significantly larger and is comparable to that of the Fe moment (45). The induced spin-polarization of Cr has been directly observed by measuring the spin-polarization of secondary electrons excited

from a (100)-oriented single crystalline Cr wedge deposited on a single crystal Fe whisker by the electron beam in a scanning electron microscope (SEMPA) (10, 44). The direction of the induced Cr moment at the surface of the Cr layer is observed to oscillate with increasing Cr thickness in a manner consistent with the variation of the interlayer magnetic coupling between Fe layers observed in related structures in which a thin Fe layer is deposited on top of the Cr wedge (46). It is the induced spin density wave in the spacer layer material that mediates the magnetic coupling of the magnetic layers in magnetic multilayers and sandwiches.

The interlayer exchange coupling of thin layers of Fe, Co, Ni, and their alloys via nonmagnetic transition and noble metal spacer layers nearly always exhibits an oscillatory variation with spacer layer thickness (25). The oscillation period varies from metal to metal and lies between $\approx 8 \text{ \AA}$ and 12 \AA in most cases, with the exception of Cr, for which it is significantly longer ($\approx 18 \text{ \AA}$). In some cases, more than one oscillation period has been observed. For Cr, a second short oscillation period just ≈ 2 monolayers long has been observed (46, 47). The interlayer coupling has been explored experimentally in many systems using a wide variety of techniques, including SEMPA and XMCD, as well as more conventional techniques including various magnetometries, Brillouin light scattering (see, for example, 48–50) and ferromagnetic resonance (51). A detailed discussion of interlayer coupling can be found elsewhere (7, 10, 38, 52–54).

A SIMPLE MODEL OF GIANT MAGNETORESISTANCE

The detailed origin of GMR has provoked considerable interest. Many theoretical models have been developed, but most of them are based on a model of the electrical conduction in ferromagnetic metals from Mott (55). Mott hypothesized that the electrical current in ferromagnetic metals is carried independently in two conduction channels that correspond predominantly to the spin-up and spin-down *s-p* electrons. These electrons are in broad energy bands with low effective masses. This assumption is believed to be good at temperatures significantly below the magnetic ordering temperature of the magnetic material so that there is little spin-mixing between the two conduction channels. Mott theorized that the conductivity can be significantly different in the two spin channels because the conduction-electron scattering rates in these two channels will be related to the corresponding spin-up or spin-down density of empty states at the Fermi level. These states will be largely of *d* character, and as a result of the exchange split *d* bands, the ratio of spin-up to spin-down density of empty states at the Fermi level can be significantly different

in the ferromagnetically ordered states of Fe, Ni, Co, and their alloys. Consequently, this leads to the possibility of substantially different mean-free paths λ^\pm and conductivities σ^\pm in the two channels. In Co, for example, the density of states at the Fermi level is ten times higher for down-spin (minority) electrons as compared with up-spin (majority) electrons (56). (For in-depth reviews see, for example, 55–58.)

Detailed theories of the giant magnetoresistance effect in magnetic multilayers have been developed (52, 59–66). However, it is beyond the scope of this short review to discuss these models in any detail, but see the detailed discussion in reference (8). The simplest model for a magnetic multilayer that results in GMR is an equivalent resistor network model (53, 64), shown schematically in Figure 4. In this model, each of the ferromagnetic and nonmagnetic spacer layers consists of two resistors corresponding to the two conductivity channels associated with the up- and down-spin electrons. In the ferromagnetic layers, the resistivity is spin-dependent, ρ_M^\pm , whereas in the spacer layers, the resistivity in the two channels is identical, ρ_S . The resistance of the multilayer is then equivalent to that of a total of eight resistors, with four resistors in each channel. The net resistivities of the two channels can be treated as resistors in parallel. Appropriately summing the resistors within a given channel is more complicated, but there are two simple cases (53). For short mean-free paths compared with the thickness of the layers, the resistors are independent and should themselves be added in parallel. Under these circumstances, it is clear that the resistance in the ferromagnetic and antiferromagnetic configurations is the same, and consequently there is no magnetoresistance defined as $\Delta R/R = (R_{AF} - R_F)/R_F$, where R_{AF} and R_F are the resistances corresponding to the AF and F configurations. Another straightforward case is when the mean-free paths are long compared with the layer thicknesses in the multilayer. Then the resistivity is an average of the resistivity of the various layers in the multilayer, in proportion to the thicknesses of the corresponding layers. Note that for the F configuration, only two resistivities must be averaged, but in the AF configuration there are four resistivities to be considered. Taking these averages, and subsequently adding the resistivities of the two spin channels in parallel, leads to $\Delta R/R = [(\alpha - \beta)^2]/[4(\alpha + N/M)(\beta + N/M)]$, where N and M are the thicknesses of the spacer and ferromagnetic layers, and $\alpha = \rho_F^+/\rho_S$ and $\beta = \rho_F^-/\rho_S$. The magnetoresistance in this model depends on two parameters, α/β and $M\beta/N$. This model shows, not surprisingly, that the magnitude of $\Delta R/R$ is strongly dependent on the scattering asymmetry between the spin conduction channels in the ferromagnetic layers. Of course it is irrelevant in which spin channel the scattering is stronger, and the magnitude of the MR depends on how much the ratio α/β differs from

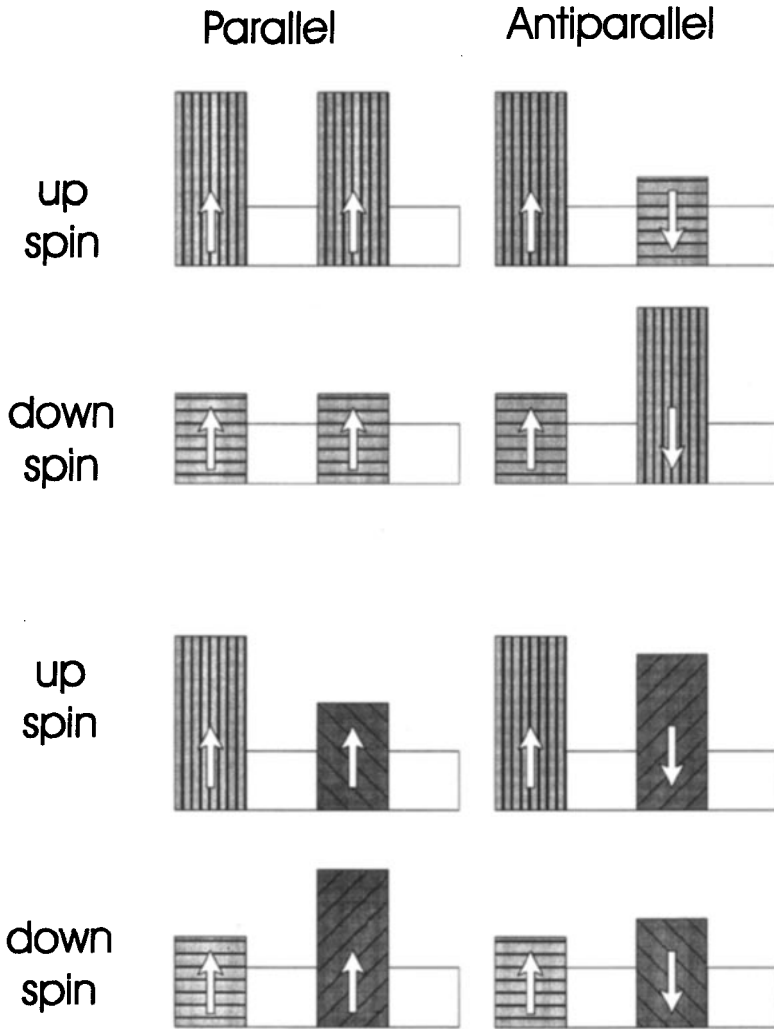


Figure 4 A simple resistor network model of GMR in which the height of the columns is proportional to the resistivity of the magnetic (*arrows*) and spacer layer (*white boxes*) metals for the two independent up- and down-spin channels. The magnetic orientation of the magnetic layers is shown by the direction of the arrow inscribed in the relevant box. Two different multilayers are considered. In the top portion of the figure, a simple multilayer containing one type of magnetic layer is described. In the bottom portion, a resistor network model is shown for a magnetic multilayer containing two different types of magnetic layers separated by the same spacer layer.

Annu. Rev. Mater. Sci. 1995.25:357-388. Downloaded from arjournals.annualreviews.org by Max-Planck-Gesellschaft on 05/06/05. For personal use only.

1. This highly simplified model also predicts that for a constant ratio α/β , the MR decreases monotonically with increasing spacer layer thickness, falling off as $1/N^2$ for large N . The MR is actually found to decrease exponentially with N for large N (67). The reason for this discrepancy is that the resistor network model is no longer applicable for N large compared to the mean-free path in the spacer layer. Such a simple resistor network model can easily give values of MR exceeding 100% for α/β ratios of ≈ 8 to 10 (13, 53), and these ratios are considered reasonable (56, 57). Nevertheless, we note that, as shown by the resistor network model, the magnitude of the MR is expected to be related to the ratio of the scattering rates within the two conduction channels no matter where the spin-dependent scattering takes place. The scattering asymmetries have been indirectly determined from measurements of the resistivity of magnetic ternary alloys (56–58). However, no correlation between the magnitude of the scattering asymmetries from studies of bulk magnetic alloys and the magnitude of the MR in magnetic multilayers has yet been found.

The simple resistor network model discussed above predicts that the resistance of a magnetic multilayer will be higher for antiparallel alignment of the magnetic layers as compared with parallel alignment. This is schematically demonstrated in the upper portion of Figure 4, where it is clear that the lower resistance for parallel alignment of the magnetic layers results from a short circuit of the current through one of the spin conduction channels (shown in the figure as the down-spin channel). A simple extension of this model can be made for the case of a ferromagnetic multilayer containing two different ferromagnetic layers with different ratios (α/β), shown in the cartoon in the lower part of Figure 4. In this case, the resistance of the multilayer will be lower for the antiparallel alignment of neighboring magnetic layers, thereby leading to a positive or an inverse giant magnetoresistance effect. This effect has not yet been unambiguously demonstrated, but the observation of a large inverse GMR effect would be important to clarify theoretical models of GMR.

INVERSE GIANT MAGNETORESISTANCE IN SPIN-ENGINEERED MULTILAYERS

The interlayer exchange coupling strength in antiferromagnetically coupled magnetic multilayers can be readily measured from the field required to rotate the magnetic moments of neighboring magnetic layers parallel to one another (68–71). Indeed, the strength of the AF interlayer coupling J_{AF} is related to the magnetization M_S and thickness t_F of the magnetic layers and the field H_S needed to rotate the magnetic moments of these layers parallel to one another, by the relation, $J_{AF} \approx H_S M_S t_F / 4$

(71, 72). It is more difficult to determine ferromagnetic coupling strengths, although these can be calculated from the stiffness of spin wave modes in ferromagnetic resonance (73) or Brillouin light-scattering studies (50). A simple technique to measure ferromagnetic coupling strengths in multilayers was developed by spin-engineering appropriate structures such that the coupling strength could be inferred directly from the magnetization vs field loop (24). The method is shown in the upper portion of Figure 5. The basic idea is to ensure that the two magnetic layers of interest (the top and middle Co layers in the example shown in Figure 5), which are ferromagnetically coupled, have their magnetic moments arranged antiparallel to one another for some field range. In Figure 5, the two uppermost Co layers are weakly ferromagnetically coupled through a spacer layer of Cu. A third Co layer (the bottom layer in the figure) is designed to be strongly antiferromagnetically coupled to the middle Co layer through a thin layer of Ru. It turns out that Co layers are coupled strongly antiferromagnetically for Ru layers a monolayer or so thick (19). Thus a structure has been spin-engineered in which at low fields the top two ferromagnetically coupled Co layers are aligned antiparallel to the applied field. This occurs because the magnetic moment of the bottom Co layer is designed to be slightly larger than the sum of the magnetic moments of the top two Co layers. Because the ferromagnetic coupling of the top two layers is much weaker in strength than the strong antiferromagnetic coupling between the bottom two Co layers, when a magnetic field is applied, the magnetic moment of the topmost Co layer rotates in the field and becomes aligned with the field for intermediate field strengths. Thus, as shown in Figure 5, the two ferromagnetically coupled Co layers become aligned antiparallel to one another. The field required to rotate the top layer in this way will be proportional to the ferromagnetic interlayer coupling strength (provided the middle Co layer remains blocked). By further increasing the applied magnetic field strength, the middle layer magnetic moment will eventually rotate parallel to the applied field. The field strength required to do this is determined primarily by the strength of the antiferromagnetic coupling of this layer to the bottom Co layer. The magnetization vs field strength of a typical Co/Ru/Co/Cu/Co sample is shown in Figure 5. It behaves exactly as described above. Similar structures have been used to measure oscillations in ferromagnetic interlayer coupling via Ru (24), Cu (74), and Pd (75).

The dependence of the resistance of the spin-engineered structure with field shown in Figure 5 is unusual. The structure does indeed exhibit GMR, but as expected from the unusual variation of the magnetic structure with field, the resistance of the structure increases for small fields. This is simply because the relative orientation of the two Co layers surrounding the Cu

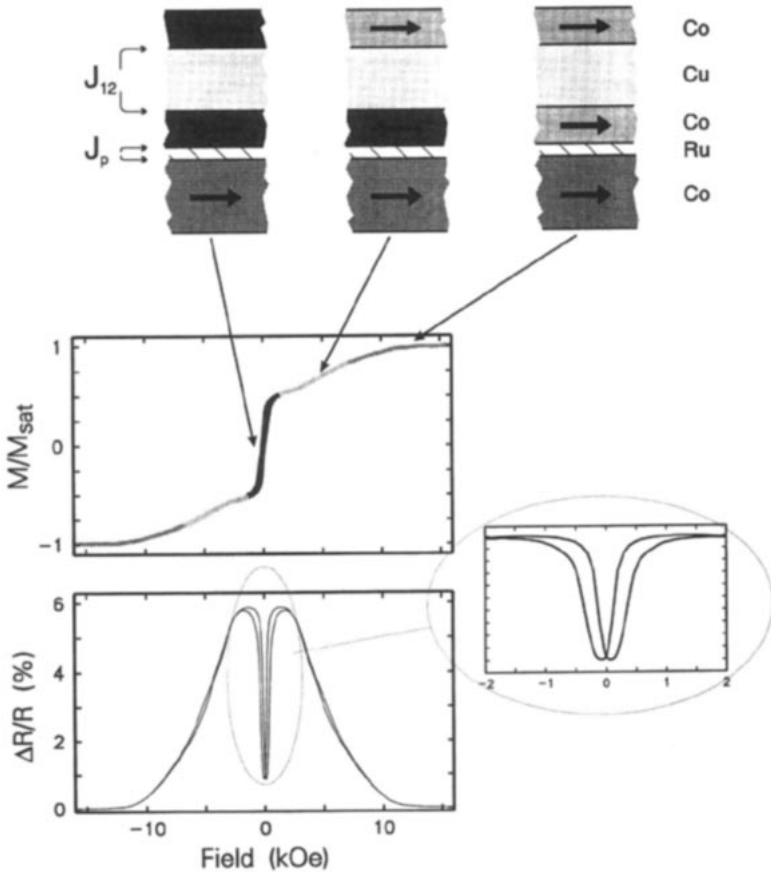


Figure 5 Schematic diagram of a spin-engineered structure in which two Co layers are ferromagnetically exchange coupled through a Cu layer of the appropriate thickness with an interlayer coupling strength J_{12} . The middle Co layer is antiferromagnetically coupled to a third (lower) Co layer through a thin Ru layer, with a coupling strength J_p . The moment of the lower Co layer is set to be equal to or slightly larger than the sum of the moments of the top two Co layers. The magnetic arrangement of the Co layers is shown for small, intermediate, and strong magnetic fields (*left, middle* and *right*, respectively). These arrangements correspond to the regions of the magnetization vs field and corresponding resistance vs field curves as indicated by the arrows. The inset at the right of the figure is an enlarged view of the low field region of the resistance vs field curve, which demonstrates an inverse GMR effect (see 24).

layer changes from being parallel to being antiparallel to one another. Thus this structure exhibits an inverse GMR effect, although its origin is simply related to the unusual field dependence of the magnetic configuration of the magnetic layers. At higher fields, the resistance of the

structure decreases as the magnetic moments of all three magnetic layers become parallel to the applied field, as shown in the figure.

GIANT MAGNETORESISTANCE AT LOW FIELDS IN MAGNETIC MULTILAYERS

For applications of giant magnetoresistance to magnetoresistive sensors for magnetic recording applications, large changes in resistance at low fields of ≈ 5 to 10 Oe are required (28). At present, the magnetoresistive component of such sensors is comprised of a thin film alloy of Ni and Fe, permalloy (Py), $\text{Ni}_{81}\text{Fe}_{19}$. Permalloy exhibits a reasonably large magnetoresistance at room temperature of nearly 4% for fields of less than 1 Oe for films of thickness $> \approx 1000 \text{ \AA}$ (11). Note, however, that the typical operating temperature in a high-capacity magnetic disk storage drive is likely to be significantly higher than room temperature, perhaps $\approx 100^\circ\text{C}$. An important stimulus to much work on GMR is to develop structures with large GMR values at the lowest possible fields. In addition to large low-field GMR, the structures must possess certain other properties if they are to be useful as MR sensors for magnetic data storage applications. These properties include magnetic stability and reproducibility; stability against the elevated temperatures required for processing of the MR device; low magnetostriction so that the material will be insensitive to strains induced during processing; stability against electromigration due to the very high current densities (10^7 to 10^8 A/cm^2) the material will experience in order to obtain the required signal; and stability against corrosion from the environment within which the material will operate. These conditions are quite stringent and difficult to meet.

Dependence of Giant Magnetoresistance on Spacer Layer Thickness

At first glance, the very large GMR values in Figure 1 are extremely promising for MR read head applications. However, the saturation fields are clearly too high for useful application to MR recording heads. As shown in Figure 2, the magnitude of the GMR decays rather slowly with increasing Cu layer thickness in Co/Cu multilayers. Indeed, the GMR decays approximately as the inverse of Cu layer thickness at low temperatures, where the mean-free path of the conduction electrons within the Cu layers is long compared to the Cu layer thickness. At higher temperatures, where the mean-free path becomes comparable to the range of Cu layer thicknesses shown in Figure 2, the GMR decays more rapidly, approximately as $\Delta R/R \propto 1/t_{\text{Cu}} \exp^{-t_{\text{Cu}}/\lambda_{\text{Cu}}}$, where t_{Cu} is the Cu layer thickness and λ_{Cu} describes scattering within the Cu layer interior (67). This

functional dependence can be understood by considering two effects. First, increasing the Cu layer thickness dilutes the interfacial scattering regions because the measuring current, which is parallel to the layers, is shunted through the bulk of the Cu layers away from these regions. Second, scattering within the interior of the Cu layers will clearly diminish the flow of electrons between Co layers. This scattering can be described by a scattering length λ_{Cu} , which is likely related to the mean-free path in thick Cu layers, where the contribution from scattering at the surfaces of the film is small. Thus, for sufficiently thick Cu layers where most of the current is carried by the Cu layers, we can account for the variation of GMR with Cu layer thickness (67). In contrast, the interlayer exchange coupling decays much more rapidly with increasing Cu layer thickness (22, 74, 76–79). For example, this means that for Cu layers about twice as thick as those contained in the Co/Cu multilayer in Figure 1, the GMR is only reduced by a factor of two, but the saturation field is about 20 times smaller. Thus GMR values of almost 35% for fields of about 100 Oe are possible for Cu layer thicknesses of $\approx 20 \text{ \AA}$ (77). Such materials may be useful for magnetic field MR sensors.

Giant Magnetoresistance in Permalloy/Au Multilayers

As mentioned above, oscillatory interlayer coupling has been observed in a wide variety of transition metal multilayers. Whereas the oscillation period is similar for many systems and there is no simple variation of the period with spacer layer material, there is a systematic variation of the interlayer coupling strength with the position of the transition metal spacer element in the periodic table. Indeed, the coupling strength is found to increase exponentially with d -band filling across the $3d$, $4d$, and $5d$ periods. In addition, the coupling strength increases systematically from the $5d$ to $4d$ to $3d$ elements in any given column of the periodic table (25). Based on these considerations and taking into account that noble metal spacer layers typically give the largest GMR values, good candidates for the large GMR at low saturation fields (low interlayer coupling) are multilayers with Au spacer layers. Indeed, one of the first observations of GMR in magnetic multilayers was in perpendicularly magnetized and magnetically weakly coupled or uncoupled Co/Au/Co sandwiches (80, 81). The two Co layers were sufficiently thin that the magnetic interface anisotropy was able to overcome the demagnetization field from the Co magnetization so that the magnetic moments were perpendicularly magnetized in zero magnetic field. By preparing the two Co layers with slightly different thicknesses, and correspondingly different magnetic perpendicular anisotropies, the moments of the two Co layers switched at different field strengths. Thus there was a certain field range where the Co moments were aligned anti-

parallel to one another. The resistance of this structure was higher than for fields where the Co moments were aligned parallel to one another. This structure is similar to subsequent observations of GMR in permalloy/Cu/Co/Cu multilayers (82) and exchange-biased sandwiches (83) in which successive magnetic layers are designed to have different in-plane coercivities or switching fields, as discussed further below.

Antiferromagnetic coupling across Au spacer layers and oscillations in the magnetic interlayer coupling with Au thickness have been observed in Fe/Au/Fe sandwiches and Fe/Au multilayers (84–87), although only small GMR values were observed (86). Recently, oscillatory coupling via Au sandwiched between Co layers (88) and permalloy layers (89) has been found. The latter system displays large MR values at very low fields at room temperature, as described below.

The magnitude of the saturation magnetoresistance vs Au layer thickness is plotted in Figure 6a for three families of (111)-oriented Py/Au multilayers. The multilayers were prepared by MBE deposition and were grown on (0001) sapphire substrates. The [111] crystalline orientation was established by using a thin Pt seed layer, $\approx 20 \text{ \AA}$ thick, grown at 600°C . Related saturation fields determined from the magnetoresistance curves are shown in Figure 6b. They correspond to the field at which the MR is half that of the saturation MR. Four well-defined oscillations in saturation magnetoresistance and saturation field are found as the Au layer thickness is increased (indicated by AF_n , $n = 1-4$ in Figure 6a). Typical resistance vs in-plane magnetic field curves are shown in Figure 7 for samples corresponding to the four maxima in Figure 6a and b. Note that a small amount of Au was deliberately inserted in the permalloy layers in two of the families of samples depicted in Figure 6, by coevaporation from the permalloy and Au sources. This was an attempt to take advantage of the likely surface-segregation of the Au from the Py layers during growth so as to reduce the possibility of magnetic pin-holes between the Py layers. Similar samples grown without Au in the Py layers show suppression of the MR peak near $t_{\text{Au}} \approx 11 \text{ \AA}$ (AF1). An analogous surfactant effect has been reported for copper surface-segregation through cobalt during epitaxy of exchange-coupled Co/Cu (111) multilayers (90). Note that alloying the permalloy with Au has little effect on the properties of the system for thicker Au layers, except that the resistivity of the multilayers is increased. For example, at the second MR peak, the resistivity is increased by about 30%, consistent with the decreased MR of these samples (see Figure 6, *open squares*) relative to otherwise similar samples.

Typical magnetization vs in-plane magnetic field are shown in Figure 8a and b for two Py/Au multilayers from the AF1 and AF2 peaks. The magnetization loops are consistent with the resistance curves shown in

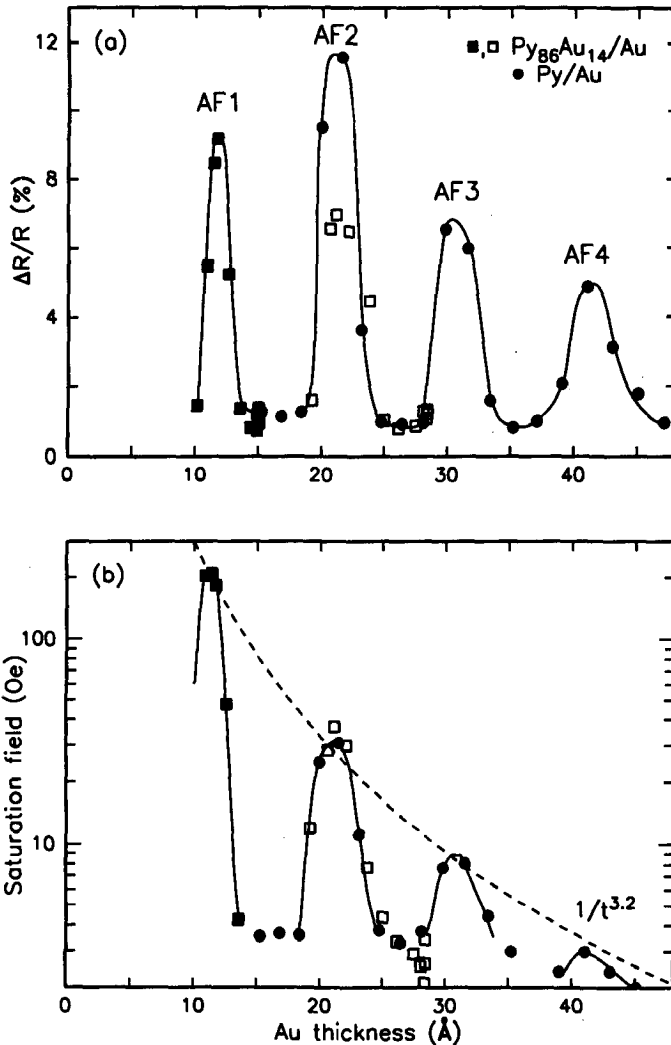


Figure 6 Room temperature saturation magnetoresistance (a) and saturation field (b) vs Au spacer layer thickness at 295 K for three series of Py/Au multilayers. The open and solid boxes correspond to two samples grown with Py₈₆Au₁₄ magnetic layers, and the solid circles correspond to samples prepared with Py layers. Four peaks in MR and saturation field are observed in the Au thickness range spanned, as indicated by AF1, AF2, AF3, and AF4 (from 89).

Figure 7 and indicate antiferromagnetic coupling of the permalloy layers. The degree of antiferromagnetic coupling can be inferred from the remanent magnetization near zero field. Figure 8 demonstrates almost perfect antiferromagnetic alignment at the AF2 peak but incomplete ($\approx 45\%$) AF

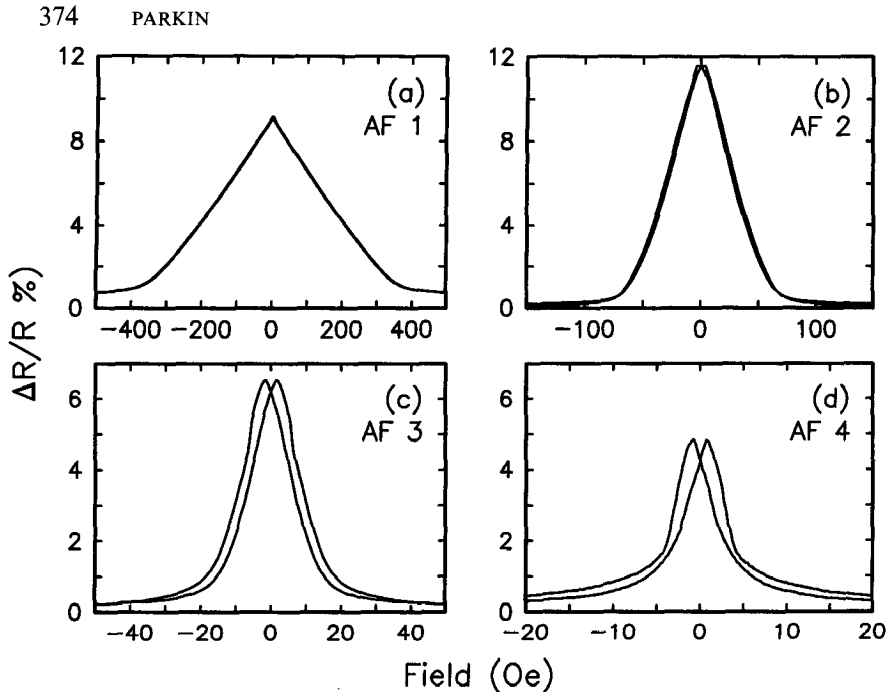


Figure 7 Room temperature resistance vs in-plane magnetic field curves for four samples corresponding to the four maxima in MR shown in Figure 6, with Au layer thicknesses of (a) AF1: 11.7 Å, (b) AF2: 21.5 Å, (c) AF3: 29.8 Å, and (d) 41.0 Å. The corresponding resistivities of these samples at room temperature are ≈ 43 , 19, 13, and 10 $\mu\text{Ohm-cm}$, respectively, in fields large enough to saturate the magnetization of the samples.

coupling at the AF1 peak. The detailed relationship of magnetization and MR is explored in Figure 8c and d. Because permalloy is a soft magnetic material whose magnetization is saturated in small fields, the simplest model of GMR can be used in which the resistance is proportional to the cosine of the angle between the magnetic moments of neighboring layers (91). Then the resistance of the structure is expected to vary as $-M(H)^2$, where $M(H)$ is the magnetization parallel to the applied field H . Figures 8b and d show a comparison of resistance and $-M^2$ vs field curves. Excellent agreement is obtained confirming the expected relationship. Note that for the AF1 sample, the MR is compared with $-(M - M_0)^2$, where M_0 is the residual magnetization in small fields. M_0 represents the portion of the sample ($\approx 55\%$) containing ferromagnetically coupled Py layers due to structural defects. These layers do not contribute to the magneto-resistance. If there were complete AF coupling of the Py layers, these data would suggest that the magnitude of the MR at the AF1 peak would be

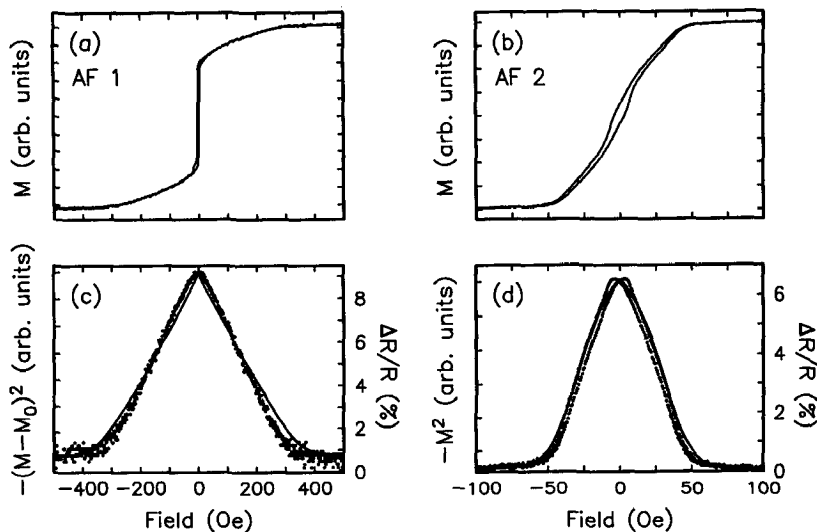


Figure 8 Magnetization vs field curves, (a) and (b), for two Py-Au/Au multilayers from the AF1 and AF2 peaks shown in Figure 6. In (c) and (d), corresponding resistance vs field curves (solid lines) and plots of $-(M - M_0)^2$ vs field (solid circles) are shown. M_0 is the remanent magnetization.

much higher ($MR \approx 20\%$) for multilayers containing Py-Au magnetic layers and yet higher still for pure Py layers.

The magnetic interlayer coupling in the Py/Au multilayers is relatively small. For example, at the AF1 peak, J_{AF} is ≈ 0.02 erg/cm². This is approximately five times larger than that found in sputtered (111) textured Py/Au multilayers (92). Although the magnitude is similar to that found in sputtered Py/Cu multilayers (93), if we assume J_{AF} is proportional to M^2 , the magnetic coupling through epitaxial (111) Au is about an order of magnitude smaller than the coupling found at AF1 in epitaxial (111) Cu (94). Note that as mentioned above for Co/Cu multilayers, the strength of the coupling falls off rapidly with thicker Au layers. Indeed, as shown in Figure 6b, the coupling varies as approximately $1/t_{Au}^n$, where $n = \approx 3.2$. Such a dependence is more rapid than predicted in simple Ruderman-Kittel-Kasuya-Yosida (RKKY) models of the coupling (95).

Interlayer coupling is usually found to be weaker in polycrystalline multilayers than in similar single crystalline multilayers. Note that the lowest reported saturation fields at room temperature in magnetic multilayers are found in sputtered Py/Au multilayers where changes in resistance of ≈ 1 to 2%/Oe can be obtained (92).

Giant Magnetoresistance in Exchange-Biased Sandwiches

An important structure for obtaining GMR at low magnetic fields is shown in Figure 9. This structure, an exchange-biased sandwich (EBS), is in its simplest embodiment, $F_I/S/F_{II}/\text{FeMn}$. The EBS contains two ferromagnetic layers, F_I and F_{II} , and a single nonmagnetic spacer layer, S , in

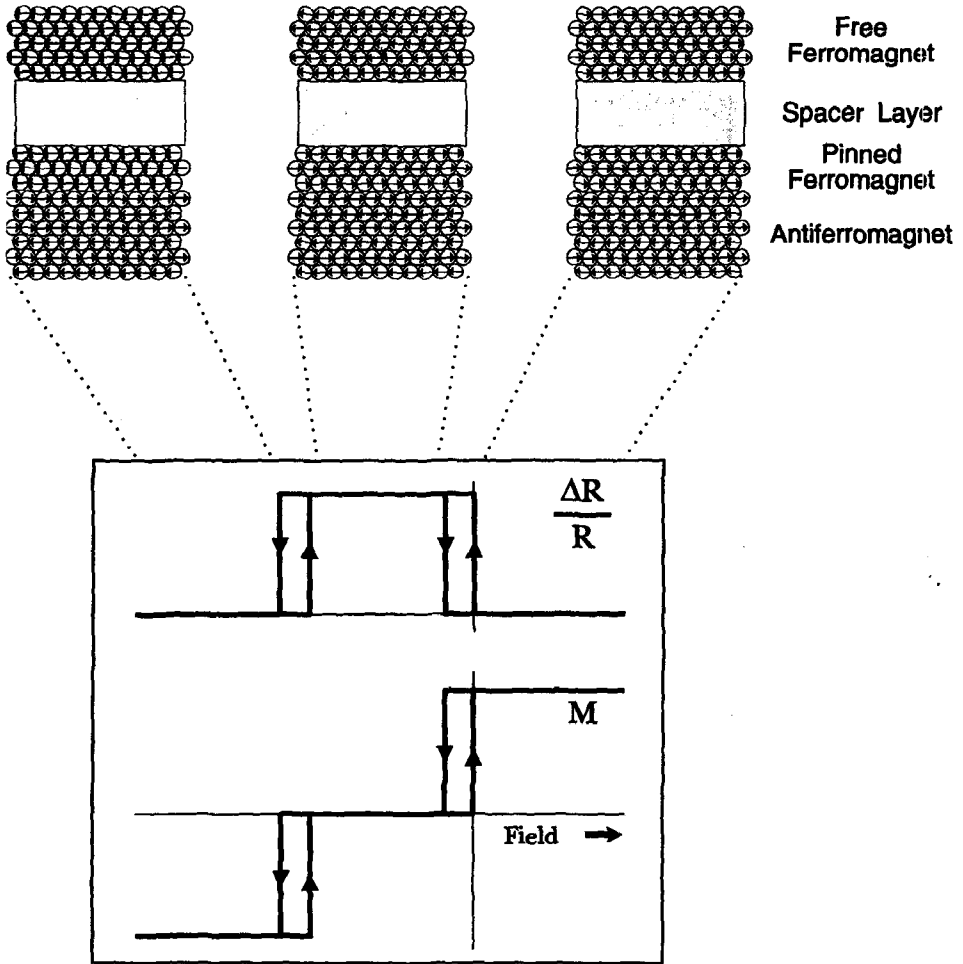


Figure 9 Schematic diagram of an exchange-biased sandwich structure.

which one of the magnetic layers, F_{II} , is exchange coupled to an antiferromagnetic layer. EBS structures with antiferromagnetic exchange bias layers of FeMn (83), NiO (96), and TbFe (97) have been reported. The structure takes advantage of a phenomenon first discovered more than 30 years ago in oxidized Co particles (98) and subsequently extensively studied in a number of thin film systems (99–101). This phenomenon, often referred to as exchange anisotropy, arises from an interfacial magnetic exchange coupling between an antiferromagnetic layer and a ferromagnetic layer. Under appropriate conditions, the exchange anisotropy results in a unidirectional anisotropy in the F layer such that its magnetic hysteresis loop is centered about a non-zero field, a bias field H_B . In contrast, providing that the magnetic coupling of F_I and F_{II} via the spacer layer is sufficiently weak, the magnetic hysteresis loop of F_I is centered close to zero field. The moments of F_I and F_{II} are thus aligned antiparallel for some field range intermediate between zero and H_B . A resistance vs field curve is shown in Figure 10*a* for a typical EBS structure, where F_I and F_{II} are Py and S is Cu. The current and field are aligned along the unidirectional anisotropy direction. The structure displays a giant MR effect exactly analogous to that in multilayers with a higher resistance for fields where F_I and F_{II} are antiparallel. As is found for multilayered structures (22, 93), replacing the Py layers with Co layers of the same thickness increases the magnetoresistance of the structure by approximately a factor of two, as shown in Figure 10*b*.

The quest for structures exhibiting large changes in resistance per unit field has motivated a great deal of work in GMR. The simplest structure with the largest change in resistance per unit field at room temperature is shown in Figure 10*c*. This structure is comprised of elements of the two EBS structures shown in Figure 10*a* and *b*. As can be seen from Figure 10*a*, the Py/Cu/Py EBS has a small switching field and values of $\Delta R/R$ of about 2–4% at room temperature. Similar Co/Cu/Cu EBS have higher MR values, as high as $\approx 9\%$ at room temperature, but larger switching fields. The increased switching field results from the higher magnetic anisotropy of Co as compared with Py. To obtain the highest values of MR per unit field, EBS sandwiches such as those shown in Figure 10*c* have been developed (102). These structures are essentially comprised of a Py/Cu/Py EBS in which thin Co layers are introduced at each Py/Cu interface. The Co layers need only be approximately 1 atomic layer thick, or just sufficient to completely cover the Py/Cu interface. These structures also dramatically demonstrate the overwhelming importance of spin-dependent scattering at the magnetic/nonmagnetic interfaces (102, 103).

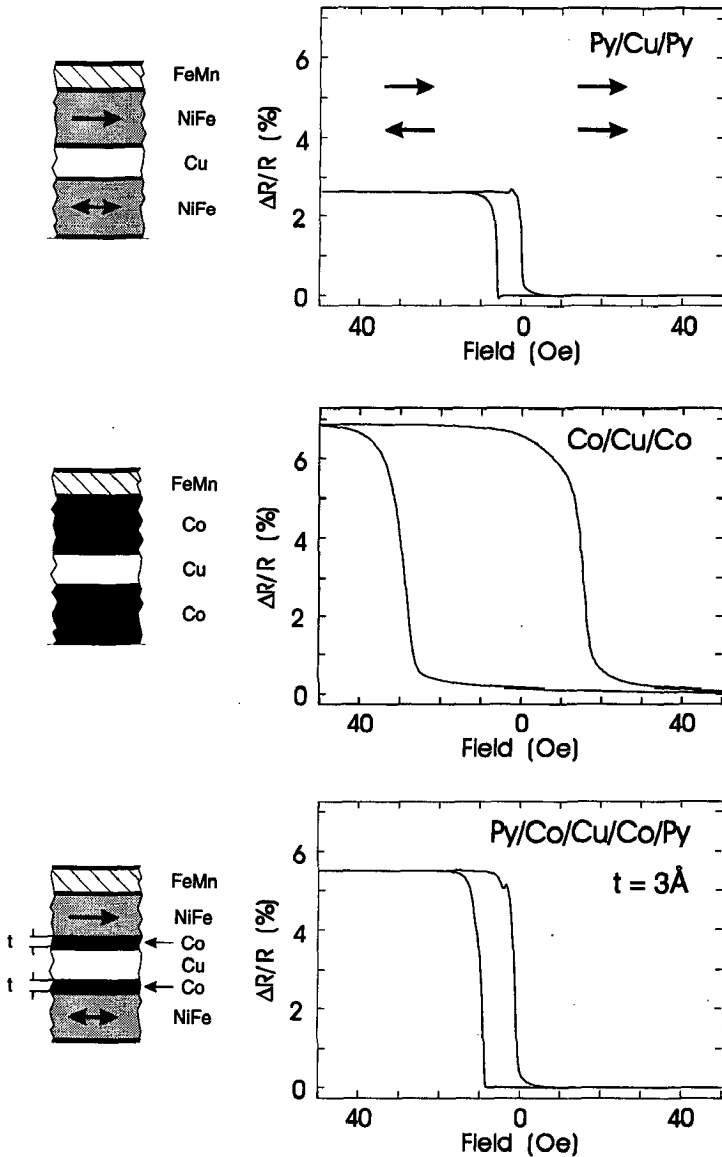


Figure 10 Room temperature resistance vs field curves for (a) Si/Py(53 Å)/Cu(32 Å)/Py(22 Å)/FeMn(90 Å)/Cu(10 Å); (b) the same structure with the Py (permalloy = Ni₈₁Fe₁₉) layers replaced by Co; and (c) the same structure as in (a) but with 3.0 Å-thick Co layers added at each Py/Cu interface. (Note the thicknesses of the Py layers have correspondingly been reduced by 3.0 Å.)

DEPENDENCE OF GIANT MAGNETORESISTANCE ON STRUCTURE

In multilayers, the magnitude of the saturation giant magnetoresistance is strongly dependent on the details of the multilayer structure. In particular, the GMR will depend on the thicknesses of both the magnetic and non-magnetic layers and the number of bilayers, as well as on the composition and thickness of any seed layers and capping layers. In addition, the GMR is sensitive to the detailed morphology of the structure, which can be changed by varying deposition conditions such as the deposition temperature, the detailed method of preparation, and the substrate. The GMR will also be decreased if the magnetic layers are not completely coupled antiferromagnetically to one another in the high resistance state. This means that it is very easy to obtain different values of GMR for nominally the same structure, and it is very difficult to make meaningful comparisons of results on individual samples from different groups. It is most useful to study sets of samples made under identical conditions where one aspect of the structure is systematically varied.

Dependence of GMR on Number of Bilayers

Perhaps one of the most obvious aspects of the structure of a magnetic multilayer that can be varied is the overall thickness of the multilayer, as determined by the number of bilayers N . The magnitude of the GMR can be, and usually is, strongly dependent on N . Figure 11 shows typical resistance vs field curves for representative samples from two series of Fe/Cr multilayers with different N . The series differ only in the thicknesses of the Cr overlayer t_o and the Cr underlayer t_u . A minimum Cr underlayer thickness of $\approx 10 \text{ \AA}$ was required for the growth of well-layered structures. As can be seen from Figure 11, the measured GMR is increased with increasing N in both series of structures. However, the rate of increase of GMR with N is significantly different for the two series. This is clearly demonstrated in Figure 12, where the detailed dependence of MR on N is displayed for the two families of structures. The magnetoresistance is observed to increase much more rapidly with N for the $[\text{Fe}/\text{Cr}]_N$ multilayers with very thin Cr under- and overlayers than for the structures with thicker Cr layers. The origin of this effect is similar to that described above for the dependence of GMR on Cu layer thickness in Co/Cu multilayers. The GMR in the Fe/Cr multilayers is reduced in proportion to the measuring current passing through the Cr under- and overlayers. The dilution of the $[\text{Fe}/\text{Cr}]_N$ portion of the multilayer contributing to the giant MR, by the noncontributing portion of the structure, will be decreased as the relative proportion of the noncontributing portion decreases with increased N .

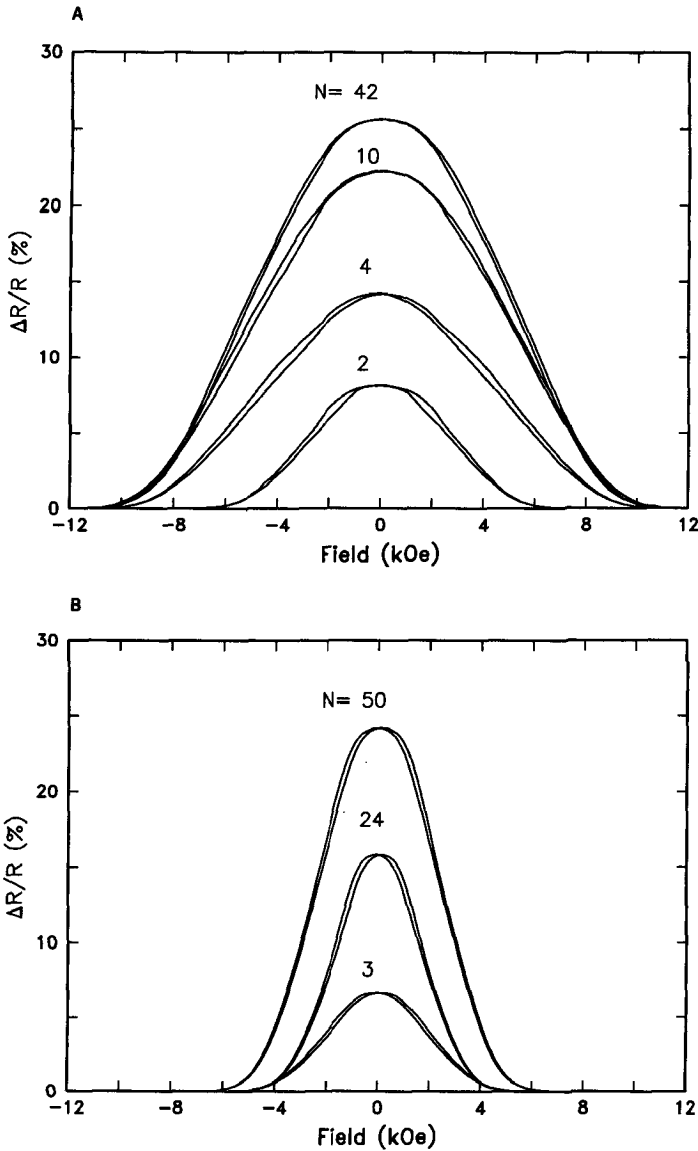


Figure 11 Resistance vs field curves at 4.2 K for several members of two families of Fe/Cr multilayers with different number of bilayers. (a) This corresponds to data for Fe/Cr multilayers of the form Si/10 Å Cr/[18 Å Fe/9 Å Cr]_N/10 Å Cr with $N = 2, 4, 10,$ and 42. (b) This corresponds to data for Si/115 Å Cr/[16 Å Fe/11.5 Å Cr]_N/115 Å Cr with $N = 3, 24,$ and 50.

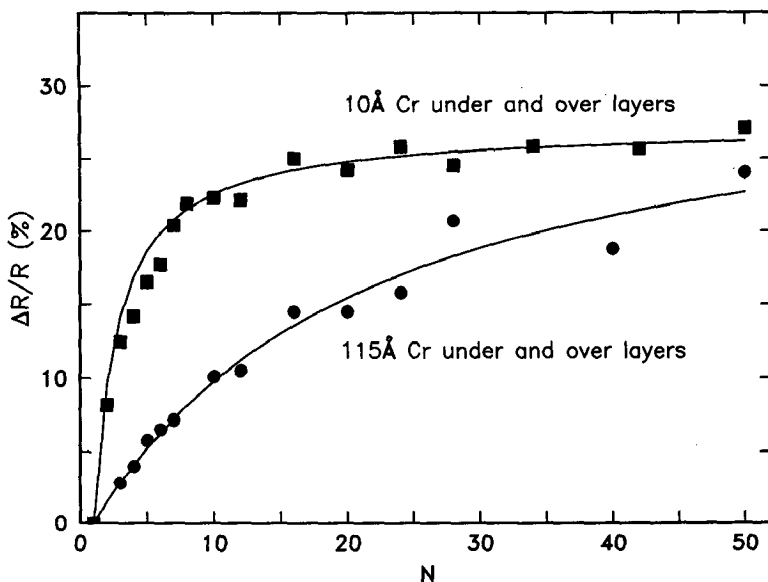


Figure 12 Dependence of saturation magnetoresistance on number of bilayers for two series of Fe/Cr multilayers with structure of the form (*upper line*) Si/10 Å Cr/[18 Å Fe/9 Å Cr]_N/10 Å Cr; and (*lower line*) Si/115 Å Cr/[16 Å Fe/11.5 Å Cr]_N/115 Å Cr.

The results shown in Figure 12 are rather similar to those found for many magnetic multilayered systems. It is not surprising, therefore, that the largest GMR values in Fe/Cr (and other multilayers) are found in multilayers with large values of N (33, 34). The dependence on N is not completely determined by a simple dilution effect; there are several other factors. First, an important and very simple factor affecting the dependence of GMR on N is that the two magnetic layers at either end of the multilayer contribute to GMR only half as much as the magnetic layers within the interior of the multilayer (assuming diffuse scattering at either extremity of the multilayer). Second, as described in the very first models of GMR (59, 61, 62), the GMR will be increased if the electrons propagate across many magnetic/nonmagnetic interfaces within a conduction carrier mean-free path. When N is small compared with some mean-free path within the multilayer, the GMR is reduced. Thus it follows that the dependence of GMR on N will be temperature dependent, as described by the temperature dependence of the mean-free path. This effect is much more important as the conductivity of the multilayer increases: for example, in multilayer systems containing metals with long mean-free paths such as Cu, Ag, and Au and in single-crystal, defect-free multilayer systems. Third,

the resistance of the film will increase as the film thickness is decreased because of scattering at the film surfaces. This leads to a decreased GMR effect.

Finally, it must be noted that the structure of the multilayer itself will vary with total film thickness. For polycrystalline films, the grain size often increases in proportion to the film thickness. The GMR is clearly sensitive to the grain size (35). The variation in number of grain boundaries with film thickness will lead to variations in film resistivity and thus GMR. For single-crystal films with no large-angle grain boundaries, the changes in structure with film thickness may be more subtle. For Fe/Cr, it has been proposed that increases in GMR with N may be attributed to an increase in the roughness of the Fe/Cr interfaces at some length scale (104). Indeed, a particularly important aspect of the origin of GMR, which is not discussed in detail in this article, is the role of the structure of the interfaces, which remains controversial.

Dependence of GMR on Magnetic Layer Thickness

A basic assumption of the resistor network model of GMR described above is that the spin-dependent scattering giving rise to the GMR originates purely within the interior of the magnetic layers, i.e. from bulk spin-dependent scattering. This model can be readily generalized to allow for spin-dependent interfacial scattering by adding additional resistors in the network representing the scattering in the interfacial regions. The relative contribution of spin-dependent scattering from bulk scattering and from spin-dependent scattering at the interfaces between the magnetic and spacer layers is a subject of great current interest.

A simple experiment to examine the role of interfacial vs bulk spin-dependent scattering is to vary the interfacial content of the magnetic multilayer by varying the thickness of the magnetic layers. Figure 13 shows various resistance vs field curves measured at 4.2 K for sets of otherwise identical Fe/Cr multilayers in which the Fe layer thickness is systematically varied from ≈ 1.5 to 300 Å. The magnitude of the saturation GMR for these samples is plotted in Figure 14 vs Fe layer thickness. These data show that maximum GMR values are obtained for thin Fe layers ≈ 8 Å-thick, which strongly suggests that interfacial scattering is of predominant importance. Note, however, that the GMR is diluted by the presence of necessary underlayers (for growth) and overlayers (for protection against corrosion). This means that the Fe thickness for which maximum GMR is obtained will be affected by the presence of these layers and by the thickness of the Cr spacer layers themselves. Increasing the thickness of these layers will increase the thickness of Fe necessary to obtain maximum

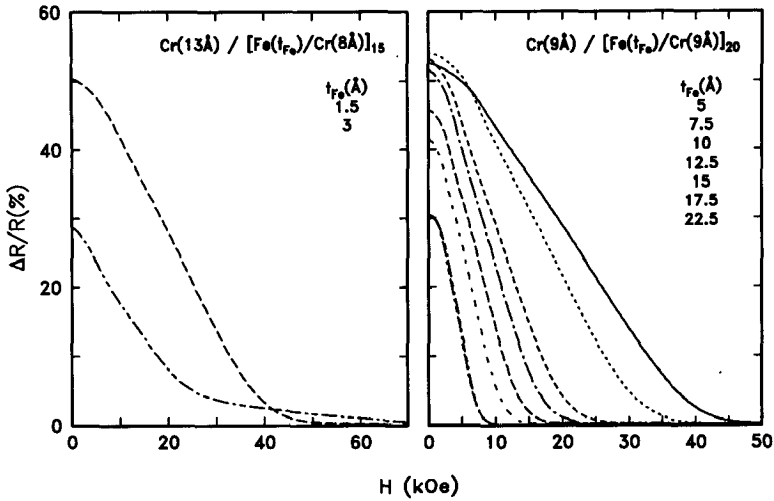


Figure 13 Resistance vs field curves for several $\text{Si}/\text{Cr}(t_u)/[\text{Fe}(t_{\text{Fe}})/9 \text{ \AA} \text{ Cr}]_{20}$ multilayers with varying Fe layer thickness t_{Fe} . The Cr underlayer thickness t_{Cr} is $\approx 10 \text{ \AA}$. On the left panel, the sample with $t_{\text{Fe}} = 1.5 \text{ \AA}$ has the smaller GMR. On the right panel, the saturation field systematically increases from the largest to the smallest value of t_{Fe} shown.

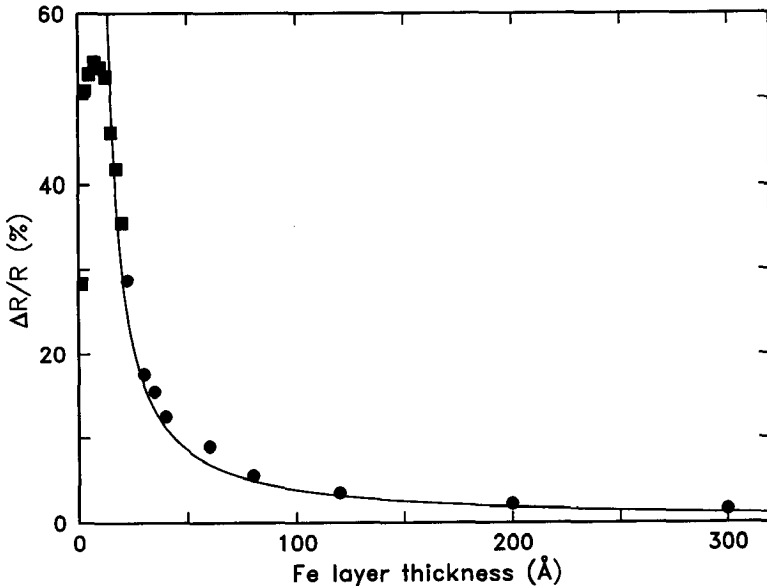


Figure 14 Dependence of saturation magnetoresistance at 4.2 K vs Fe layer thickness for structures $\text{Si}/9 \text{ \AA} \text{ Cr}/[\text{Fe}(t_{\text{Fe}})/9 \text{ \AA} \text{ Cr}]_{20}$, for Fe layer thicknesses ranging from 1.5 to 300 Å. For thick Fe layers, the anisotropic magnetoresistance (AMR) becomes a significant fraction of the GMR effect. For these samples, shown as filled circles, the AMR was measured and a correction applied.

GMR. Thus it is not straightforward to interpret such studies without appealing to detailed theoretical models. Note, however, that GMR models predict a maximum in the GMR effect for Fe layers significantly thicker than those found in Figure 14 for any significant spin-dependent bulk scattering (105). Finally, note that the MR decreases approximately as the inverse Fe layer thickness for Fe layers, ranging in thickness from 20 to 300 Å, consistent with dilution of the interfacial scattering regions, and predominant interfacial spin-dependent scattering. Similarly, in granular alloys, the magnitude of GMR decreases approximately as the inverse size of the magnetic particles, as shown in Figure 15.

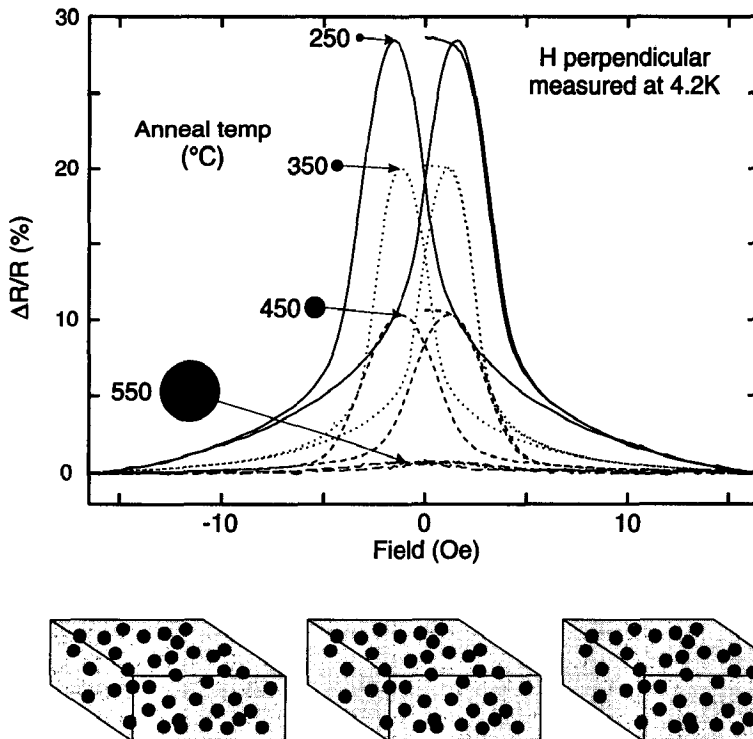


Figure 15 Variation of GMR in a single crystal (111) $\text{Co}_{28}\text{Cu}_{72}$ granular alloy at 4.2 K with annealing temperature of the alloy. The granular alloy was deposited at 200°C and successively annealed for 1 h at 250, 350, 450, and 500°C. The size of the Co particles as determined from small-angle grazing incidence X-ray scattering is shown by the size of a representative particle. Note that the largest particle size for the sample annealed at 550°C is ≈ 135 Å (see 115 for more details).

CONCLUSIONS

Interest in magnetic nano-structured metals has substantially increased in recent years with the discovery of giant magnetoresistance and oscillatory interlayer exchange coupling in magnetic multilayers and related structures. This brief review has discussed only a small amount of the published work in this field, which continues to grow at an enormous pace. Important omissions include work on detailed models of interlayer coupling and GMR; magnetotransport in magnetic multilayers and sandwiches in which the current flows perpendicular to the layers (31, 32, 106–110); the detailed role of the influence of the structural morphology, especially of the interfaces, on GMR; detailed discussions of magnetic granular alloys and multilayered granular structures (42); spin-dependent quantum confinement of electrons in the magnetic potentials created by the magnetic/nonmagnetic interfaces; and the influence of such potentials on the interlayer coupling and GMR (see, for example, PD Johnson, this volume). Magnetic nano-structures display other anomalous transport properties including giant magneto-thermopower and giant magneto-thermal conductivities (see, for example, 111), which have not been discussed herein.

It seems quite clear that giant magnetoresistance is intimately related to scattering at the interfaces between the magnetic and nonmagnetic components in both magnetic-layered structures and granular alloys. The largest GMR values are usually found for structures in which the interfacial component is maximized, by reducing either the thickness of magnetic layers or the size of the magnetic particles. Similarly, the GMR is extremely sensitive to the detailed chemical nature of the interfaces. Modifications of these interfaces by dusting with just sub-monolayer to monolayer equivalent coverages of impurity elements results in dramatic variations in GMR values (102). Indeed, GMR may thus be used to probe the electronic character of the magnetic/nonmagnetic interfaces, just as oscillatory interlayer coupling can be used to probe details of the Fermi surface topology of the spacer layer material (38, 52) and perhaps the magnetic layer material (112–114). The ability to tailor-make magnetic nano-structured materials with properties especially engineered for particular applications is very attractive and is likely to lead to important applications for such structures in the near future.

ACKNOWLEDGMENTS

I would like to thank many colleagues, especially Drs. R F C Farrow, R Marks, A R Modak and Prof. D J Smith for their contributions to parts

of the work described in this paper. I am especially grateful to Kevin Roche for technical support.

Any *Annual Review* chapter, as well as any article cited in an *Annual Review* chapter, may be purchased from the Annual Reviews Preprints and Reprints service.
1-800-347-8007; 415-259-5017; email: arpr@class.org

Literature Cited

1. Schuller IK, Falco CM. 1982. *Prog. Phys.* 4: 492
2. Schuller IK. 1988. In *Physics, Fabrication, and Applications of Multilayered Structures*, ed. P Dhez, C Weisbuch, p. 139. New York: Plenum
3. Falicov LM, Pierce DT, Bader SD, Gronsky R, Hathaway KB, et al. 1990. *J. Mater. Res.* 5: 1299
4. Mathon J. 1991. *J. Magn. Magn. Mater.* 100: 527
5. Fert A, Bruno P. 1994. See Ref. 116, p. 82
6. Hathaway KB. 1994. See Ref. 116, p. 45
7. Heinrich B, Cochran JF. 1993. *Adv. Phys.* 42: 523
8. Levy PM. 1994. In *Solid State Physics*, ed. H Ehrenreich, D Turnbull, 47: 367. New York: Academic
9. Parkin SSP. 1994. See Ref. 116, p. 148
10. Pierce DT, Unguris J, Celotta RJ. 1994. See Ref. 116, p. 117
11. McGuire TR, Potter RI. 1975. *IEEE Trans. Magn.* MAG-11: 1018
12. Binash G, Grünberg P, Saurenbach F, Zinn W. 1989. *Phys. Rev. B* 39: 4828
13. Baibich MN, Broto JM, Fert A, Nguyen van Dau F, Petroff F, et al. 1988. *Phys. Rev. Lett.* 61: 2472
14. Grünberg P, Schreiber R, Pang Y, Brodsky MB, Sowers H. 1986. *Phys. Rev. Lett.* 57: 2442
15. Carbone C, Alvarado SF. 1987. *Phys. Rev. B* 36: 2443
16. Joyce BA. 1985. *Rep. Prog. Phys.* 48: 1637
17. Ploog K. 1988. *Angew. Chem. Int. Ed. Engl.* 27: 5931
18. Farrow RFC, Marks RF, Harp GR, Weller D, Rabedeau TA, et al. 1993. *Mater. Sci. Eng. Rep.* R11: 155
19. Parkin SSP, More N, Roche KP. 1990. *Phys. Rev. Lett.* 64: 2304
20. Parkin SSP, York BR. 1993. *Appl. Phys. Lett.* 62: 1842
21. Parkin SSP, Li ZG, Smith DJ. 1991. *Appl. Phys. Lett.* 58: 2710
22. Parkin SSP, Bhadra R, Roche KP. 1991. *Phys. Rev. Lett.* 66: 2152
23. Kano H, Kagawa K, Suzuki A, Okabe A, Hayashi K, Aso K. 1993. *Appl. Phys. Lett.* 63: 2839
24. Parkin SSP, Mauri D. 1991. *Phys. Rev. B* 44: 7131
25. Parkin SSP. 1991. *Phys. Rev. Lett.* 67: 3598
26. Kryder MH. 1993. *Annu. Rev. Mater. Sci.* 23: 411
27. Grochowski E, Thompson DA. 1994. *IEEE Trans. Magn.* 30: 3797
28. Ciureanu P. 1992. In *Thin Film Resistive Sensors*, ed. P Ciureanu, S Middehoek, p. 253. Bristol: IOP Pub.
29. Daughton JM. 1992. *Thin Solid Films* 216: 162
30. Prinz G. 1990. *Science* 250: 1092
31. Johnson M. 1993. *Science* 260: 320
32. Johnson M. 1993. *Appl. Phys. Lett.* 63: 1435
33. Fullerton EE, Conover MJ, Mattson JE, Sowers CH, Bader SD. 1993. *Appl. Phys. Lett.* 63: 1698
34. Schad R, Potter CD, Belien P, Verbanck G, Moshchalkov VV, Bruynseraede Y. 1994. *Appl. Phys. Lett.* 64: 3500
35. Modak AR, Smith DJ, Parkin SSP. 1994. *Phys. Rev. B*, 50: 4232
36. Parkin SSP, Roche KP, Suzuki T. 1992. *Jpn. J. Appl. Phys.* 31: L1246
37. Johnson MT, Coehoorn R, de Vries JJ, McGee NW, aan de Stegge J, Bloemen PJ. 1992. *Phys. Rev. Lett.* 69: 969
38. Bruno P, Chappert C. 1992. *Phys. Rev. B* 46: 261
39. Berkowitz AE, Mitchell JR, Carey MJ, Young AP, Zhang S, et al. 1992. *Phys. Rev. Lett.* 68: 3745
40. Xiao JQ, Jiang JS, Chien CL. 1992. *Phys. Rev. Lett.* 68: 3749
41. Parkin SSP, Farrow RF, Rabedeau TA, Marks RF Harp GR, et al. 1993. *Eur. Phys. Lett.* 22: 455
42. Hylton TL, Coffey KR, Parker MA, Howard JK. 1993. *Science* 261: 1021
43. Samant MG, Stör J, Parkin SSP, Held GA, Hermsmeier BD, et al. 1994. *Phys. Rev. Lett.* 72: 1112

44. Unguris J, Celotta RJ, Pierce DT. 1992. *Phys. Rev. Lett.* 69: 1125
45. Pappas DP, Prinz GA, Ketchen MB. 1994. *Appl. Phys. Lett.* 65: 3401
46. Unguris J, Celotta RJ, Pierce DT. 1991. *Phys. Rev. Lett.* 67: 140
47. Purcell ST, Folkerts W, Johnson MT, McGee NW, Jager K, et al. 1991. *Phys. Rev. Lett.* 67: 903
48. Demokritov SO, Tsymbal E. 1994. *J. Phys. Condens. Matter* 6: 7145
49. Cochran JF. 1994. See Ref. 116, p. 223
50. Hillebrands B, Güntherodt G. 1994. See Ref. 116, p. 258
51. Krebs JJ, Lubitz P, Chaiken A, Prinz GA. 1989. *Phys. Rev. Lett.* 63: 1645
52. Edwards DM, Mathon J, Muniz RB, Phan MS. 1991. *Phys. Rev. Lett.* 67: 493
53. Mathon J. 1991. *Contemp. Phys.* 32: 143
54. Stiles MD. 1993. *Phys. Rev. B* 48: 7238
55. Mott NF. 1964. *Adv. Phys.* 13: 325
56. Campbell IA, Fert A. 1982. In *Ferromagnetic Materials*, ed. EP Wohlfarth, 3: 747. Amsterdam: North-Holland
57. Dorleijn JW. 1976. *Philips Res. Rep.* 31: 287
58. Rossiter PL. 1987. *The Electrical Resistivity of Metals and Alloys*, Cambridge: Cambridge Univ. Press
59. Camley RE, Barnas J. 1989. *Phys. Rev. Lett.* 63: 664
60. Levy PM, Ounadjela K, Zhang S, Wang Y, Sommers CB, Fert A. 1990. *J. Appl. Phys.* 67: 5914
61. Barnas J, Fuss A, Camley RE, Grünberg P, Zinn W. 1990. *Phys. Rev. B* 42: 8110
62. Barthelemy A, Fert A. 1991. *Phys. Rev. B* 43: 13124
63. Inoue J, Oguri A, Maekawa S. 1991. *J. Phys. Soc. Jpn.* 60: 376
64. Edwards DM, Muniz RB, Mathon J. 1991. *IEEE. Trans. Mag.* 27: 3548
65. Trigui F, Velu E, Dupas C. 1991. *J. Magn. Magn. Matter* 93: 421
66. Zhang S, Levy PM, Fert A. 1992. *Phys. Rev. B* 45: 8689
67. Parkin SSP, Modak AR, Smith DJ. 1993. *Phys. Rev. B* 47: 9136
68. Barthelemy A, Fert A, Baibich MN, Hadjoudj S, Petroff F, et al. 1990. *J. Appl. Phys.* 67: 5908
69. Dieny B, Gavigan JP, Rebouillat JP. 1990. *J. Phys. Condens. Matter* 2: 159
70. Dieny B, Gavigan JP. 1990. *J. Phys. Condens. Matter* 2: 187
71. Folkerts W. 1991. *J. Magn. Magn. Matter* 94: 302
72. Parkin SSP, Mansour A, Felcher GP. 1991. *Appl. Phys. Lett.* 58: 1473
73. Heinrich B. 1994. See Ref. 116, p. 195
74. Bloemen PJH, van Dalen R, de Jonge WJM, Johnson MT, aan de Stegge J. 1993. *J. Appl. Phys.* 73: 5972
75. Bloemen PJH, de Jonge WJM, Donkersloot HC. 1993. *J. Appl. Phys.* 73: 4522
76. Cebollada A, Miranda R, Schneider CM, Schuster P, Kirschner J. 1991. *J. Magn. Magn. Matter* 102: 25
77. Parkin SSP. 1992. In *Magnetic Surfaces, Thin Films and Multilayers*, ed. SSP Parkin, H Hopster, J-P Renard, T Shinjo, W Zinn, 231: 211. Pittsburgh: Mater. Res. Soc. Symp. Proc.
78. Johnson MT, Purcell ST, McGee NW, Coehoorn R, aan de Stegge J, Hoving W. 1992. *Phys. Rev. Lett.* 68: 2688
79. Qiu ZQ, Pearson J, Bader SD. 1992. *Phys. Rev. B* 46: 8659
80. Velu E, Dupas C, Renard D, Renard JP, Seiden J. 1988. *Phys. Rev. B* 37: 668
81. Dupas C, Beauvillain P, Chappert C, Renard JP, Trigui F, et al. 1990. *J. Appl. Phys.* 67: 5680
82. Shinjo T, Yamamoto H. 1990. *J. Phys. Soc. Jpn.* 59: 3061
83. Dieny B, Speriosu VS, Parkin SSP, Gurney BA, Wilhoit DR, Mauri D. 1991. *Phys. Rev. B* 43: 1297
84. Fuss A, Demokritov S, Grünberg P, Zinn W. 1992. *J. Magn. Magn. Matter* 103: L221
85. Marty A, Gilles B, Eymery J, Chamberod A, Joud JC. 1993. *J. Magn. Magn. Matter* 121: 57
86. Shintaku K, Hosoito N, Shinjo T. 1993. *J. Magn. Magn. Matter* 121: 413
87. Sato H, Kobayashi Y, Aoki Y, Shintaku K, Hosoito N, Shinjo T. 1993. *J. Phys. Soc. Jpn.* 62: 3380
88. Grolier V, Renard D, Bartenlian B, Beauvillain P, Chappert C, Dupas C, Ferre J, Galtier M, Kolb E, Mulloy M, Renard JP, Veillet P. 1993. *Phys. Rev. Lett.* 71: 3023
89. Parkin SSP, Farrow RFC, Marks RF, Cebollada A, Harp GR, Savoy R. 1994. *Phys. Phys. Lett.* 72: 3718
90. Harp GR, Parkin SSP, Farrow RFC, Marks RF, Toney MF, Lam QH, Rabedeau TA, Savoy RJ. 1993. *Phys. Rev. B* 42: 8721
91. Chaiken A, Prinz GA, Krebs JJ. 1990. *J. Appl. Phys.* 67: 4892
92. Parkin SSP, Rabedeau TA, Farrow RFC, Marks R. 1994. *J. Appl. Phys.* 76: 6617
93. Parkin SSP. 1992. *Appl. Phys. Lett.* 60: 512
94. Parkin SSP, Marks RF, Farrow RFC, Harp GR, Lam QH, Savoy RJ. 1992. *Phys. Rev. B* 46: 9262

95. Roth LM, Zeiger HJ, Kaplan TA. 1966. *Phys. Rev.* 149: 519
96. Anthony TC, Brug JA, Zhang, S. 1994. *IEEE Trans. Mag.* 30: 3819
97. Freitas PP, Leal JL, Melo LV, Oliveira NJ, Rodrigues L, Sousa AT. 1994. *Appl. Phys. Lett.* 65: 403
98. Meiklejohn WH, Bean CP. 1959. *Phys. Rev. B* 102: 1413
99. Yelon A. 1971. In *Physics of Thin Films: Advances in Research and Development*, ed. M Francombe, R. Hoffman, 6: 205. New York: Academic
100. Tsang C, Lee K. 1982. *J. Appl. Phys.* 53: 2605
101. Parkin SSP, Deline V, Hilleke R, Felcher GP. 1990. *Phys. Rev. B* 42: 10583
102. Parkin SSP. 1993. *Phys. Rev. Lett.* 71: 1641
103. Parkin SSP. 1992. *Appl. Phys. Lett.* 61: 1358
104. Fullerton EE, Kelly DM, Guimpel J, Schuller IK, Bruynseraede Y. 1992. *Phys. Rev. Lett.* 68: 859
105. Levy PM, Zhang S, Fert A. 1990. *Phys. Rev. Lett.* 65: 1643
106. Pratt WP, Lee SF, Slaughter JM, Loloee R, Schroeder PA, Bass J. 1991. *Phys. Rev. Lett.* 66: 3060
107. Lee SF, Pratt WP, Loloee R, Schroeder PA, Bass J. 1993. *Phys. Rev. B* 46: 548
108. Yang Q, Holody P, Lee S-F, Henry LL, Loloee R, Schroeder PA, et al. 1994. *Phys. Rev. Lett.* 72: 3274
109. Gijs MA, Giesbers JB, Lenczowski SK, Janssen HH. 1993. *Appl. Phys. Lett.* 63: 111
110. Gijs MA, Lenczowski SK, van de Veerdonk RJ, Giesbers JB, Johnson MT, aan de Stegge JB. 1994. *Phys. Rev. B* 50: 16733
111. Shi J. 1994. *Magneto-transport properties of giant magnetoresistive systems*. PhD thesis. Univ. Illinois, Urbana
112. Bruno P. 1993. *Eur. Phys. Lett.* 23: 615
113. Bloemen PJH, Johnson MT, van de Vorst MT, Coehoorn R, de Vries JJ, et al. 1994. *Phys. Rev. Lett.* 72: 764
114. Okuno SN, Inomata K. 1994. *Phys. Rev. Lett.* 72: 1553
115. Rabedeau TA, Toney M, Marks RF, Parkin SSP, Farrow RFC, Harp G. 1993. *Phys. Rev. B* 48: 16810
116. Heinrich B, Bland JAC, eds. 1994. *Ultrathin Magnetic Structures*, Vol. 2. Berlin: Springer-Verlag



CONTENTS

ELECTRONIC STRUCTURE THEORY IN THE NEW AGE OF COMPUTATIONAL MATERIALS SCIENCE, <i>Arthur J. Freeman</i>	1
DENSITY FUNCTIONAL THEORY AS A MAJOR TOOL IN COMPUTATIONAL MATERIALS SCIENCE, <i>Arthur J. Freeman,</i> <i>Erich Wimmer</i>	7
MOLECULAR ORBITAL MODELS OF SILICA, <i>L. L. HENCH, J. K. WEST</i>	37
MODELING THE DEVELOPMENT AND RELAXATION OF STRESSES IN FILMS, <i>M. D. Thouless</i>	69
LASER-BEAM INTERACTION WITH DEFECTS ON SEMICONDUCTOR SURFACES: An Approach to Production of Defect-Free Surfaces, <i>Noriaki Itoh, Jyun'ichi Kanasaki, Akiko Okano, Yasuo Nakai</i>	97
MAGNETISM AND GIANT MAGNETO-TRANSPORT PROPERTIES IN GRANULAR SOLIDS, <i>C. L. Chien</i>	129
SYNTHESIS OF POROUS SILICATES, <i>M. M. Helmkamp, M. E. Davis</i>	161
THE NATURE OF GRAIN BOUNDARIES IN THE HIGH T_C SUPERCONDUCTORS, <i>S. E. Babcock, J. L. Vargas</i>	193
▷ LASER-INDUCED PHASE TRANSITIONS IN SEMICONDUCTORS, <i>Y. Siegal, E. N. Glezer, L. Huang, E. Mazur</i>	223
PHASE TRANSITIONS IN III-V COMPOUNDS TO MEGABAR PRESSURES, <i>Arthur L. Ruoff, Ting Li</i>	249
FERROELECTRIC THIN FILMS FOR PHOTONICS: Properties and Applications, <i>D. Dimos</i>	273
THE ULTIMATE STRENGTH AND STIFFNESS OF POLYMERS, <i>Buckley Crist</i>	295
INTERFACES BETWEEN INCOMPATIBLE POLYMERS, <i>Manfred Stamm,</i> <i>Dirk Wolfram Schubert</i>	325
GIANT MAGNETORESISTANCE, <i>S. S. P. Parkin</i>	357
▷ EPITAXY OF DISSIMILAR MATERIALS, <i>C. J. Palmström</i>	389

▷ GeSi/Si NANOSTRUCTURES, <i>E. A. Fitzgerald</i>	417
SPIN POLARIZED PHOTOEMISSION, <i>P. D. Johnson</i>	455
▷ FULLERENES AND FULLERENE-DERIVED SOLIDS AS ELECTRONIC MATERIALS, <i>M. S. Dresselhaus, G. Dresselhaus</i>	487
▷ METALORGANIC CHEMICAL VAPOR DEPOSITION OF OXIDE THIN FILMS FOR ELECTRONIC AND OPTICAL APPLICATIONS, <i>Bruce W. Wessels</i>	525
▷ LOW-TEMPERATURE GROWN III-V MATERIALS, <i>M. R. Melloch, J. M. Woodall, E. S. Harmon, N. Otsuka, Fred H. Pollak, D. D. Nolte, R. M. Feenstra, M. A. Lutz</i>	547
▷ LUMINESCENCE AS A DIAGNOSTIC OF WIDE-GAP II-VI COMPOUND SEMICONDUCTOR MATERIALS, <i>B. J. Skromme</i>	601
▷ METAL-OXIDE HETEROSTRUCTURES, <i>R. Ramesh, V. G. Keramidas</i>	647
▷ HIGH-TEMPERATURE SUPERCONDUCTING MULTILAYERS AND HETEROSTRUCTURES GROWN BY ATOMIC LAYER-BY-LAYER MOLECULAR BEAM EPITAXY, <i>J. N. Eckstein, I. Bozovic</i>	679
▷ WIDE BANDGAP II-VI HETEROSTRUCTURES FOR BLUE/GREEN OPTICAL SOURCES: Key Materials Issues, <i>Leslie A. Kolodziejski, Robert L. Gunshor, Arto V. Nurmikko</i>	711
INDEXES	
Subject Index	755
Cumulative Index of Contributing Authors, Volumes 21–25	766
Cumulative Index of Chapter Titles, Volumes 21–25	768
▷ Keynote Topic: Electronic Materials	